A Note on Certain Perturbation Methods for Solving the Problem of Fully Developed Flow Through a Porous Channel

Ali R. Ansari*† Helmi Temimi ‡ Mariam Kinawi§ Abdul Majeed Siddiqui¶

Abstract—**In this paper, the recently developed Optimal Homotopy Asymptotic Method (OHAM) is applied to the problem of flow through a porous channel where the flow entry profiles are taken to be PoiseuilleCouette combinations. Analytical as well numerical solutions for the velocity profiles of the resulting differential equations are obtained. Comparison with existing results reveal that the OHAM is an effective and easy to use technique for solving nonlinear problems.**

Keywords: Porous media, Optimal Homotopy Asymptotic Method, Optimal Homotopy Asymptotic Method, non-linear, porous channel.

1 Introduction

The recent past has seen an abundance of papers considering newer asymptotic methods relying on the concept of Poincrés Homotopy from abstract algebra. The two primary methods Homotopy Analysis Method (HAM) [2] and Homotopy Perturbation Method (HPM) [3] have been successful in their own right as good methods for solving nonlinear problems. The HPM in the recent past has received some criticism regarding its convergence criteria or lack thereof. Although recently [4] has shed some light on the convergence of the method. The HAM is much more stable in this regard and has been shown to be very successful in solving nonlinear problems. The attractive feature of the HPM is its ease of application, this is usually typical of algorithms used for computational solutions, where many times accuracy is compromised for speed, leading to some instabilities. All in all the HPM is still a usable method and can be employed to produce some useful results. However, since the solution produced by all these methods are power series solutions in essence, convergence can be an issue.

The focus of the current paper is to consider a more recent predecessor to this method, referred to as the Optimal Homotopy Asymptotic Method or OHAM [5]. This method is most attractive from a mathematical point of view as it has the convergence criteria built into the method similar to the HAM, but much more flexible. In this paper we will use this method to solve a well established problem in porous media. The authors have solved the same problem earlier using the HPM [6] and the results obtained were found to be acceptable when compared to other documented solutions. Here, our intention is to employ the OHAM and compare the results with the results of [1] and a bench mark numerical solution. We note that all three approaches lead to very similar results. Our aim is to show the usability of the OHAM as a powerful efficient method for solving nonlinear problems; we also, weakly by example, show that the HPM is a useful method and should not be discarded.

We now turn to the problem under consideration. As mentioned earlier the problem chosen is from the realm of the study of flow through porous media. This area itself has received considerable attention due to its many faceted practical applications. In irrigation processes, the movement of fertilizers, pollutants and nutrients into plants are all examples of flow through porous media. The study of the interaction of oil, gas and water through the porous earth layers has become more important because of the increasing demands for energy. It has also found applications in the biological sciences, particularly in biomechanics. One such application is in the human lungs, which are idealized as layers of flocs and other types of porous materials (cf. [7]).

The flow of a fluid through a porous medium is essentially a two-phase flow that consists of the flow of a matrix particle phase and a fluid phase. However, the particle

*Manuscript received March 10, 2010

†Ali R. Ansari is an Associate Professor of Mathematics and Head of Department of Mathematics & Natural Sciences at the Gulf University for Science & Technology, P.O. Box 7207, Hawally 32093, Kuwait, Email: ansari.a@gust.edu.kw.

‡Helmi Temimi is an Assistant Professor of Mathematics within the department of Mathematics & Natural Sciences in the Gulf University for Science & Technology, P.O. Box 7207, Hawally 32093, Kuwait, (corresponding author) Phone: +965-9912-3969, Fax: +965-2530-7030, Email: temimi.h@gust.edu.kw.

§Mariam Kinawi is Graduate student at Kuwait University and a Teaching Assistant in the department of Mathematics & Natural Sciences at the Gulf University for Science & Technology P.O. Box 7207, Hawally 32093, Kuwait, Email: Kinawi.M@gust.edu.kw.

¶Abdul Majeed Siddiqui is a Professor of Mathematics in the Department of Mathematics at Pennsylvania State University, York Campus, Pennsylvania State University, York, PA 17403, USA, Email: ams5@psu.edu.

phase is usually considered as a solid matrix which is rigid and hence assumed to be stationary. Therefore, effectively, the flow through the porous matrix boils down to the flow of a single phase fluid. The importance of such flows is clear from some of the applications mentioned at the onset. Solutions of the problems are of fundamental importance.

In this paper we consider one such model of fully-developed flow through a porous medium, between parallel plates, where the governing equation is the well known Darcy-Forchheimer-Brinkman equation. The entry profiles are taken to be Poiseuille, Couette and Poiseuille-Couette type. It is well known that the said equation is nonlinear and usually solved by numerical methods [1]. Here we intend to solve this problem using OHAM. This technique is relatively new and few references to date are available demonstrating its ability in successfully solving nonlinear differential equations in different fields of applied mathematics.

Therefore, in essence our paper takes an established worthwhile problem [1], and presents an analytical solution to the problem that in the past has been solved numerically. We offer verification of the solution by reducing it to the simpler Darcy-Lapwood-Brinkman model and showing that the solution reduces correctly as well. We also compare the solutions for the three scenarios of entry flows to an accurate numerical solution. We also offer an error analysis compared to the benchmark numerical solution showing the convergence of OHAM. The problem we set up consists of very general boundary conditions.

2 Problem Formulation

We start with the basic fact that the flow of a viscous fluid is governed by the continuity and the Navier Stokes equations which, when the fluid is incompressible and the flow is steady, take the form

$$\nabla \cdot \mathbf{v} = 0, \tag{1}$$

$$\rho(\mathbf{v}\cdot\nabla)\mathbf{v} = -\nabla p + \mu\nabla^2\mathbf{v}, \tag{2}$$

In (1) and (2), $\mathbf{v}$ is the velocity vector, μ is the viscosity, ρ is the density and p is the pressure. In accordance with the averaging approach of [7] we express the conservation of mass principle as a macroscopic continuity equation, which is similar to (1). The macroscopic momentum equations, depending on the type of the porous medium and the flow under consideration, can be expressed through the following general equation, [7]:

$$\rho\left\{\chi[\zeta-1]+1\right\}(\mathbf{v}\cdot\nabla)\mathbf{v} = -\nabla p + \mu_{\text{eff}}\left\{\chi[\vartheta-1]+1\right\}\nabla^2\mathbf{v} - \chi\left\{\frac{\mu}{k}\mathbf{v} + \frac{\rho C_d}{\sqrt{k}}\mathbf{v}|\mathbf{v}|\right\} \tag{3}$$

where $\mathbf{v}$ is the velocity vector, p is the fluid pressure, ρ is the fluid density, μ is the fluid viscosity, μ_{eff} is the viscosity of the fluid in the porous medium, $\vartheta = \mu_{\text{eff}}/\mu$, k is the permeability, C_d is the drag coefficient, ζ and χ are both binary parameters that take the values 0 and 1. Note that when $\chi = 0$, (3) reduces to the Navier Stokes equation (2); when $\chi = 1$, the flow is in the porous medium, of course the various types of porous media can be specified by the choice of the parameter ζ, [7].

In the analysis of this paper we consider the flow to be in two dimensions, hence (3) takes the following component form

$$\rho\left\{\chi[\zeta-1]+1\right\}(uu_x+vu_y) - p_x + \mu_{\text{eff}}\{\chi[\vartheta-1] +1\}\nabla^2 u - \chi\left\{\frac{\mu}{k}u + \rho C_d u\sqrt{\frac{u^2+v^2}{k}}\right\}, \tag{4}$$

$$\rho\left\{\chi[\zeta-1]+1\right\}(uv_x+vv_y) - p_y + \mu_{\text{eff}}\{\chi[\vartheta-1] +1\}\nabla^2 v - \chi\left\{\frac{\mu}{k}v + \rho C_d v\sqrt{\frac{u^2+v^2}{k}}\right\}. \tag{5}$$

We will consider the flow to be plane, parallel and fully-developed through a straight channel, this means that

$$u = u(y); \quad p = p(x);$$

$$u_x = u_{xx} = v = v_x = v_{xx} = p_y = 0. \tag{6}$$

The relations (6), automatically satisfy the continuity equation (1) and the y-momentum equation (5), and reduce the x-momentum equation (4) to

$$-p_x + \mu_{\text{eff}}\left\{\chi[\vartheta-1]+1\right\}u_{yy} - \chi\left\{\frac{\mu}{k}u + \frac{\rho C_d u|u|}{\sqrt{k}}\right\} = 0. \tag{7}$$

We introduce a characteristic length L and a free-stream characteristic velocity U_∞, these enable us to non-dimensionalise (7) employing the definitions

$$x^* = x/L, \quad y^* = y/L \quad u^* = u/U_\infty, \quad k^* = k/L^2. \tag{8}$$

Substituting (8) in (7), eliminating the asterisks and rearranging, (7) takes the following dimensionless form when $\mu = \mu_{\text{eff}}$:

$$\left\{\chi[\vartheta-1]+1\right\}u_{yy} = RC + \chi\left\{\frac{u}{k} + \frac{RC_d}{\sqrt{k}}u^2\right\} \tag{9}$$

where $C = \dfrac{p_X}{(\rho U_\infty)^2}$ and the Reynolds number $R = \dfrac{\rho U_\infty L}{\mu}$.

At this point we get more specific since we are interested in the *Darcy-Forchheimer-Brinkman* equation, taking $\chi = \vartheta = 1, \zeta = 0$, and introducing $\kappa = 1/\sqrt{k}$ we have

$$u_{yy} = RC + \kappa^2 u + RC_d\kappa u^2. \tag{10}$$

We assume the following boundary conditions

$$u(0) = a, \quad u(1) = b \tag{11}$$

where a and b simply take values either 0 or 1. These boundary conditions give us a lot of flexibility, allowing us to represent the different entry profiles that are of interest to us. The cases we will explore are:

1. For Poiseuille flow we have $a = b = 0$ and $C \neq 0$.

2. For Couette flow we have $a = 0$ and $b = 1$, with $C = 0$.

3. For Poiseuille-Couette flow we again set $a = 0$ and $b = 1$, with $C \neq 0$

In the succeeding section we will solve the more general problem keeping the boundary conditions as (11).

3 Formulation of the Optimal Homotopy Asymptotic Method (OHAM)

In this section we look at the basic idea of the OHAM. We start by classifying the equation to be solved into various components, *i.e.*,

$$L\left(u\left(x\right)\right)+N\left(u\left(x\right)\right)+g\left(x\right)=0, \quad B\left(u,\frac{du}{dx}\right)=0 \tag{12}$$

where x denotes the independent variable, $u(x)$ is an unknown function, $g(x)$ is a known function, L is a linear operator, N is a non-linear operator and B is a boundary operator. Next we introduce $p \in [0,1]$ as an embedding parameter, such that we get the following family of equations:

$$\begin{aligned}(1-p)[L\left(\phi(x,p)\right)+g(x)] = H(p)[L\left(\phi(x,p)\right)+g(x),\\ +N\left(\phi(x,p)\right)]B\left(\phi(x,p),\frac{d\phi(x,p)}{dx}\right)=0,\end{aligned} \tag{13}$$

where $\phi(x,p)$ is an unknown function and $H(p)$ is a non-zero auxiliary function for $p \neq 0$ given as

$$H(p) = pC_1 + p^2C_2 + p^3C_3 + \ldots \tag{14}$$

where $H(p) = 0$ if $p = 0$, and where $C_1, C_2, C_3, \ldots$ are constants which we will compute later. From equation (13), when $p = 0$ and $p = 1$, we have

$$\phi(x,0) = u_0(x), \quad \phi(x,1) = u(x) \tag{15}$$

respectively, which means that as p increases from 0 to 1, the solution $\phi(x,p)$ varies from $u_0(x)$ to $u(x)$. If we put $p = 0$ in equation (13), then

$$L\left(u_0(x)\right)+g(x)=0, \quad B\left(u_0(x),\frac{du_0(x)}{dx}\right)=0. \tag{16}$$

Combining (14) and (13) gives us the solution

$$\phi(x,p,C_i) = u_0(x) + \sum_{k\geq 1} u_k(x,C_i)p^k, \quad i = 1,2,3,\ldots \tag{17}$$

which is the Taylor series of $\phi(x,p)$ with respect to p, and where $u_k(x,C_i)$ can be defined as

$$u_k(x,C_i) = \frac{1}{k!}\frac{\partial^k\phi(x,p,C_i)}{\partial p^k}\bigg|_{p=0}, \quad k \geq 1, i = 1,2,3,\ldots,k. \tag{18}$$

To generate the *Zeroth-Order Problem*, we simply put $p = 0$ into equation (13), which leads to equation(16). Similarly, to generate the *First-Order Problem*, we need to differentiate equation (13) with respect to p and let $p = 0$. Thus the resultant equation will be[1]:

$$L\left(u_1(x)\right) = C_1N_0\left(u_0(x)\right), \quad B\left(u_1(x),\frac{du_1(x)}{dx}\right)=0. \tag{19}$$

Following this procedure we generate the m^{th}*-Order Problem*, by differentiating the $(m-1)^{th}$*-Order Problem* with respect to p, dividing it by $m!$ and letting $p = 0$, thus giving us

$$\begin{aligned}L\left(u_k(x)-u_{k-1}(x)\right) = C_kN_0\left(u_0(x)\right)\\ +\sum_{j=1}^{k-1}C_j\left[L\left(u_{k-j}(x)\right)+N_{k-j}\left(u_0(x),\ldots,u_{k-j}(x)\right)\right],\\ k=2,3,\ldots,B\left(u_k(x),\frac{du_k(x)}{dx}\right)=0\end{aligned} \tag{20}$$

where,

$$\begin{aligned}N_m\left(u_0(x),u_1(x),\ldots,u_{k-j}(x)\right) = \frac{1}{(m-1)!}\\ \frac{\partial^{m-1}N(\phi(x,p))}{\partial p^{m-1}}\bigg|_{p=0}.\end{aligned} \tag{21}$$

It should be emphasized that u_k for $k \geq 0$ are governed by the linear equations (16),(19),(20) and (21) with the linear boundary conditions that are derived from the original problem, and can be easily solved.

The convergence of series (17) depends on the values of C_i. If convergence occurs when $p = 1$, then we have

$$u(x,C_i) = u_0(x) + \sum_{k\geq 1} u_k(x,C_i). \tag{22}$$

Now, the solution of equation(12) should be as follows:

$$u^{(m)}\left(x,C_i\right) = u_0(x) + \sum_{k=1}^{m} u_k\left(x,C_i\right), \quad i = 1,2,\ldots,m, \tag{23}$$

where C_m is a function of x. Substituting equation(23) in equation (12) results in the expression for the residual,

[1] Another way to calculate the *First-Order Problem* and the next m^{th}*-Order Problems* is to substitute equation (17) into equation (13) and equating the coefficients of like powers of p

for $i = 1, 2, \ldots, m$

$$\Re\left(x, C_i\right) = L\left(u^{(m)}\left(x, C_i\right)\right) + N\left(u^{(m)}\left(x, C_i\right)\right) + g\left(x\right). \tag{24}$$

If $R\left(x, C_i\right) = 0$, then $u^{(m)}\left(x, C_i\right)$ will be the exact solution. Yet, since such a case will not exist for most nonlinear problems, then we can minimize the functional

$$J(C_1, C_2, \ldots, C_m) = \int_a^b \Re^2(x, C_1, C_2, \ldots, C_m)dx \tag{25}$$

where a and b are values that depend on the given problem. To get the values of C_1, C_2,C_3,..., we solve the following equations:

$$\frac{\partial J}{\partial C_1} = \frac{\partial J}{\partial C_2} = \cdots = \frac{\partial J}{\partial C_m} = 0. \tag{26}$$

By knowing the values of C_i, we can get an approximate solution for the given problem.

4 Solution of the Problem Using OHAM

Here, we will use the basic ideas mentioned in the previous section in order to solve the problem specified in equation (10). To get started, we have to re-write equation(10) in the form of equation (12), along with the boundary conditions mentioned in (10). This means that we will have

$$L\left(u\left(y\right)\right) = u^{''} - \kappa^2 u,$$
$$N\left(u\left(y\right)\right) = -RC_d\kappa u^2,$$

and

$$g\left(y\right) = -RC. \tag{27}$$

According to equation (13), and by applying OHAM, we will have the following:

$$(1-p)[\phi^{''}(y,p) - \kappa^2\phi(y,p) - RC] = H(p)[\phi^{''}(y,p)$$
$$-\kappa^2\phi(y,p) - RC - RC_d\kappa\phi^2(y,p)] \tag{28}$$

along with the following boundary conditions:

$$\phi(0,p) = a, \quad \phi(1,p) = b. \tag{29}$$

4.1 The Zeroth-Order Problem

To get the *Zeroth-Order Problem*, we need to substitute $p = 0$ into equation (28). Thus, we get the simpler ODE given as

$$u_0^{''} - \kappa^2 u_0 = RC \tag{30}$$

with boundary conditions

$$u_0(0) = a, \quad u_0(1) = b, \tag{31}$$

which gives the solution

$$u_0(y) = \alpha_0 e^{\kappa y} + \beta_0 e^{-\kappa y} - \frac{RC}{\kappa^2} \tag{32}$$

where

$$\alpha_0 = a + \frac{RC}{\kappa^2} - \beta_0 \tag{33}$$

and

$$\beta_0 = \frac{1}{2\sinh(\kappa)}\left[ae^{\kappa} - b + \frac{RC}{\kappa^2}(e^{\kappa} - 1)\right]. \tag{34}$$

4.2 The First-Order Problem

In order to get the *First-Order Problem*, we need first to differentiate (28) w.r.t the embedded parameter p. After putting $p = 0$, we get

$$u_1^{''} - \kappa^2 u_1 = -\lambda\kappa RC_d u_0^2, \tag{35}$$

subject to the boundary conditions

$$u_1(0) = 0, \quad u_1(1) = 0. \tag{36}$$

Where λ, denoted by C_1 in equation (19), is the variable used to minimize the residual $\Re$ in (24). The 1st order solution using (32) is given as

$$u_1(y) = A_1 e^{\kappa y} + B_1 e^{-\kappa y} + C_1 e^{2\kappa y} + D_1 e^{-2\kappa y}$$
$$+E_1 y e^{\kappa y} + F_1 y e^{-\kappa y} + G_1, \tag{37}$$

where

$$A_1 = \frac{1}{2\sinh(\kappa)}[C_1(e^{-\kappa} - e^{2\kappa}) + D_1(e^{-\kappa} - e^{-2\kappa})$$
$$-E_1 e^{\kappa} - F_1 e^{-\kappa} + G_1(e^{-\kappa} - 1)],$$
$$B_1 = \frac{1}{2\sinh(\kappa)}[C_1(e^{2\kappa} - e^{\kappa}) + D_1(e^{-2\kappa} - e^{\kappa})$$
$$+E_1 e^{\kappa} + F_1 e^{\kappa} + G_1(1 - e^{\kappa})],$$
$$C_1 = -\frac{RC_d\lambda\alpha_0^2}{3\kappa^2}, \quad D_1 = -\frac{RC_d\lambda\beta_0^2}{3\kappa^2},$$
$$E_1 = \frac{R^2CC_d\lambda\alpha_0}{\kappa^3}, \quad F_1 = -\frac{R^2CC_d\lambda\beta_0}{\kappa^3}$$

and

$$G_1 = \frac{RC_d\lambda}{\kappa^2}\left(2\alpha_0\beta_0 + \frac{R^2C^2}{\kappa^2}\right)$$

Next, in order to find λ, we let

$$\Re(y) = L(\tilde{u}) + g(y) + N(\tilde{u}) \tag{38}$$

where $\tilde{u} = u_0 + u_1$ is the *first-order* solution and u_0 and u_1 are given by (32) and (37). Finally, we need to minimize $J = \int_0^1 \Re^2 dy$ with respect to λ, i.e.,

$$\frac{\partial J}{\partial \lambda} = \int_0^1 2\Re\frac{\partial \Re}{\partial \lambda}dy = 0.$$

5 The finite element benchmark solution

As a benchmark, we will refer to the numerical solution given by the finite element method (FEM). We apply the FEM to the Darcy-Forchheimer-Brinkman equation

$$u_{yy} - \kappa^2 u - \kappa R C_d u^2 = RC \tag{39}$$

subject to the following boundary conditions

$$u_1(0) = a, \quad u_1(1) = b \tag{40}$$

We solve (39) using a uniform mesh with $\Delta y = 0.01$ and degree of approximation $p = 4$. Therefore, based on the well-known finite element analysis results with an $\mathcal{L}^2-$rate of convergence, we proceed with

$$||u - U_{FEM}||_{\mathcal{L}^2(0,1)} = O(\Delta y^{p+1}) \tag{41}$$

where u is the solution of (39), U_{FEM} the respective FEM solution and

$$||f||_{\mathcal{L}^2(0,1)} = \left(\int_0^1 f^2 dy \right)^{\frac{1}{2}}.$$

Then, (41) leads to the following order of accuracy

$$||u - U_{FEM}||_{\mathcal{L}^2(0,1)} = O(10^{-8}) \tag{42}$$

In the next section we provide the resulting analytical solutions of the Darcy-Forchheimer-Brinkman equation using (OHAM) for different types of entry profiles compared to the benchmark solution given by the FEM.

6 Results and Discussion

For practical purposes, we introduce three different entry flow profiles. As mentioned earlier we consider Poiseuille, Couette and Poiseuille-Couette flows. In the next few subsections, we provide the numerical and the approximate analytical solution with error discussion in the $\mathcal{L}^2$-norm.

6.1 The Darcy-Lapwood-Brinkman Equation

Mathematically, the particular form of the Darcy-Forchheimer-Brinkman equation (10), is a more general equation in the sense that it includes the microscopic inertial terms, and the Darcy-Lapwood-Brinkman equation is a particular case of the Darcy-Forchheimer-Brinkman equation (10). This particular case occurs when the drag coefficient, $C_d = 0$, reducing (10) to

$$u_{yy} = RC + \kappa^2 u, \tag{43}$$

which is the Darcy-Lapwood-Brinkman equation for the problem under consideration. Consequently, the solution of the Darcy-Lapwood-Brinkman problem is the *zeroth-order* solution for the Darcy-Forchheimer-Brinkman problem which was given by (32) hence

$$u(y) = \alpha_0 e^{\kappa y} + \beta_0 e^{-\kappa y} - \frac{RC}{\kappa^2} \tag{44}$$

where recall that α_0 and β_0 are given as in (33) and (34).

6.2 Poiseuille Entry Profile

In the first instance, we consider the Darcy-Forchheimer-Brinkman equation, we assume an entry profile of Poiseuille type by setting $a = b = 0$ and $C \neq 0$, then the solution will be given by

$$\tilde{u}(y) = u_0 + u_1 \tag{45}$$

where

$$u_0(y) = \frac{RC}{\kappa^2} \left[\alpha_0 e^{\kappa y} + \beta_0 e^{-\kappa y} - 1 \right] \tag{46}$$

$$u_1(y) = A_1 e^{\kappa y} + B_1 e^{-\kappa y} + C_1 e^{2\kappa y} + D_1 e^{-2\kappa y} + E_1 y e^{\kappa y} + F_1 y e^{-\kappa y} + G_1 \tag{47}$$

where

$$\alpha_0 = 1 - \beta_0, \quad \beta_0 = \frac{1}{2\sinh(\kappa)} (e^{\kappa} - 1)$$

and

$$A_1 = \frac{1}{2\sinh(\kappa)} [C_1(e^{-\kappa} - e^{2\kappa}) + D_1(e^{-\kappa} - e^{-2\kappa}) - E_1 e^{\kappa} - F_1 e^{-\kappa} + G_1(e^{-\kappa} - 1)]$$

$$B_1 = \frac{1}{2\sinh(\kappa)} [C_1(e^{2\kappa} - e^{\kappa}) + D_1(e^{-2\kappa} - e^{\kappa}) + E_1 e^{\kappa} + F_1 e^{\kappa} + G_1(1 - e^{\kappa})]$$

$$C_1 = -\frac{RC_d \lambda \alpha_0^2}{3\kappa^2}, \quad D_1 = -\frac{RC_d \lambda \beta_0^2}{3\kappa^2},$$

$$E_1 = \frac{R^2 C C_d \lambda \alpha_0}{\kappa^3}, \quad F_1 = -\frac{R^2 C C_d \lambda \beta_0}{\kappa^3}$$

and

$$G_1 = \frac{RC_d \lambda}{\kappa^2} \left(2\alpha_0 \beta_0 + \frac{R^2 C^2}{\kappa^2} \right). \tag{48}$$

For $C = -5$, $R = 1$, $\kappa = 1$ and $C_d = 0.55$, and using error minimization previously established in the description of (OHAM), we obtain

$$\lambda = -0.95206989754.$$

Hence the OHAM solution is given as

$$\tilde{u}(y) = 5.42216508792366e^{y} + 5.16871342119284e^{-y} + 0.31562083827832e^{2y} + 2.33214008003005e^{-2y} - 3.52070168295991ye^{y} + 9.57025940821510ye^{-y} - 18.23863942742488 \tag{49}$$

Similarly, for the Darcy-Lapwood-Brinkman equation (43) for an entry profile of Poiseuille type we substitute $a = b = 0$ and $C \neq 0$ in (45) and (48) we get

$$u(y) = \alpha_0 e^{\kappa y} + \beta_0 e^{-\kappa y} - \frac{RC}{\kappa^2} \tag{50}$$

with $\alpha_0 = 1 - \beta_0, \quad \beta_0 = \frac{1}{2\sinh(\kappa)}\left(e^{\kappa} - 1\right)$ which can be re-written as

$$u(y) = -RCk + RCk[e^{y/\sqrt{k}} + \frac{e^{y/\sqrt{k}} - e^{-y/\sqrt{k}}}{e^{1/\sqrt{k}} - e^{-1/\sqrt{k}}}$$

$$-\frac{e^{(1+y)/\sqrt{k}} - e^{(1-y)/\sqrt{k}}}{e^{1/\sqrt{k}} - e^{-1/\sqrt{k}}}] \tag{51}$$

This is in fact the exact solution of the Darcy-Lapwood-Brinkman equation [1] for a Poiseuille entry profile.

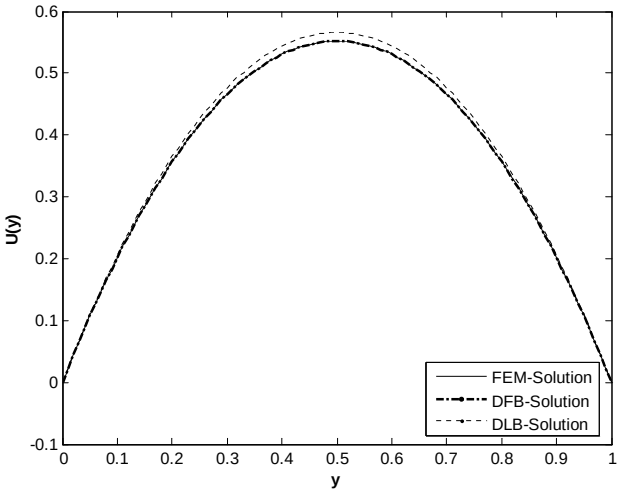

Figure 1: This graph represents a Poiseuille type entry profile. Variation of velocity u versus y for both the Darcy-Lapwood-Brinkman (DLB) and Darcy-Forchheimer-Brinkman (DFB) models. In addition, the benchmark FEM solution is also shown. For computing these graphs we have set $C = -5, R = 1$ and $k = 1$. In addition, for the DFB model $C_d = 0.55$ and for the DLB model $C_d = 0$.

In Fig. 1, we see the velocity profiles for the Darcy-Lapwood-Brinkman and Darcy-Forchheimer-Brinkman models for a Poiseuille entry profile. We clearly see that the inclusion of the microscopic inertia through the Darcy-Forchheimer-Brinkman model causes a slowing down of the flow, this is the same result obtained by [1]. These graphs also offer a verification for the solutions obtained here compared to the FEM solution as a benchmark.
In addition, Table 1 illustrates the $\mathcal{L}^2$-norm of the error between the *zeroth-order* and *first-order* solutions and the FEM-benchmark solution. We can see that the error is decreasing with respect to the order of the OHAM solution and therefore the optimal homotopy perturbation method provides a good approximation of the exact solution.

6.3 Poiseuille–Couette Entry Profile

Once again starting with the Darcy-Forchheimer-Brinkman equation, assuming an entry profile of Poiseuille–Couette type we set $a = 0, b = 1$ and $C \neq 0$ giving us the solution

$$\tilde{u}(y) = u_0 + u_1 \tag{52}$$

where

$$u_0(y) = \alpha_0 e^{\kappa y} + \beta_0 e^{-\kappa y} - \frac{RC}{\kappa^2}, \tag{53}$$

$$u_1(y) = A_1 e^{\kappa y} + B_1 e^{-\kappa y} + C_1 e^{2\kappa y} + D_1 e^{-2\kappa y} + E_1 y e^{\kappa y} + F_1 y e^{-\kappa y} + G_1, \tag{54}$$

where

$$\alpha_0 = \frac{RC}{\kappa^2} - \beta_0, \quad \beta_0 = \frac{1}{2\sinh(\kappa)}\left[\frac{RC}{\kappa^2}\left(e^{\kappa} - 1\right) - 1\right]$$

and the constants A_1, B_1, C_1, D_1, E_1, F_1 and G_1 are defined by (48). For $C = -5$, $R = 1$, $\kappa = 1$ and $C_d = 0.55$, then using error minimization previously established in the description of (OHAM) method, we obtain

$$\lambda = -0.924126564469$$

Hence the (OHAM) solution becomes

$$\tilde{u}(y) = 4.45372603492625e^{y} + 4.10178821886339e^{-y} + 0.14316548105164e^{2y} + 2.82132608622532e^{-2y} - 2.33612922296385ye^{y} + 10.37061103848490ye^{-y} - 16.52000582106661 \tag{55}$$

As one would expect the analytical solution obtained in the previous section of the Darcy-Forchheimer-Brinkman (10) should reduce to the solution of the Darcy–Lapwood–Brinkman equation (43). If we substitute $C_d = 0$ into (48) and (52) we get

$$u(y) = \frac{1}{2\sinh(\kappa)}\left[\frac{RC}{\kappa^2}\left(1 - e^{-\kappa}\right) + 1\right]e^{\kappa y} + \frac{1}{2\sinh(\kappa)}\left[\frac{RC}{\kappa^2}\left(e^{\kappa} - 1\right) - 1\right]e^{-\kappa y} - \frac{RC}{\kappa^2} \tag{56}$$

Table 1: The $\mathcal{L}^2$-norm of the error between the FEM-solution and OHAM-solutions for Poiseuille type entry profile.

Δy	0.01
Approximation degree p	4
$\|\|U_{FEM} - u_0\|\|_{\mathcal{L}^2(0,1)}$	0.02649
$\|\|U_{FEM} - \tilde{u}\|\|_{\mathcal{L}^2(0,1)}$	2.55515e-004

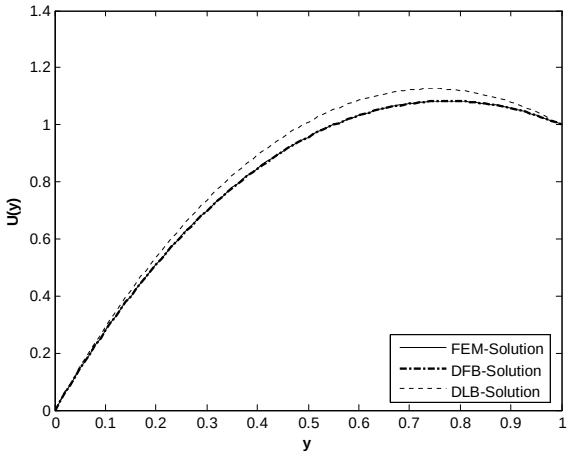

Figure 2: This graph represents a Poiseuille–Couette type entry profile. Variation of velocity u versus y for both the Darcy-Lapwood-Brinkman (DLB) and Darcy-Forchheimer-Brinkman (DFB) models. In addition, the benchmark FEM solution is also shown. For computing these graphs we have set $C = -5, R = 1$ and $k = 1$. In addition, for the DFB model $C_d = 0.55$ and for the DLB model $C_d = 0$.

which matches the result of [1] as expected. It is also worth noting that Darcy–Lapwood–Brinkman equation is a linear differential equation and simple to solve and the solution indeed is correct. In Fig. 2, we present the graphs of the solutions for the two models. Once again we notice the slower profile of the Darcy-Forchheimer-Brinkman model, due to the presence of the microscopic inertia. The graph matches closely with the results of [1]. Table 2 illustrates the $\mathcal{L}^2$-norm of the error between the *zeroth-order* and *first-order* solutions and the FEM-benchmark solution. We can see that the error is decreasing with respect to the order of the OHAM solution and therefore the optimal homotopy perturbation method provides a good approximation of the exact solution.

Table 2: The $\mathcal{L}^2$-norm of the error between the FEM-solution and OHAM-solutions for Poiseuille–Couette type entry profile.

Δy	0.01
Approximation degree p	4
$\|\|U_{FEM} - u_0\|\|_{\mathcal{L}^2(0,1)}$	0.02649
$\|\|U_{FEM} - \tilde{u}\|\|_{\mathcal{L}^2(0,1)}$	2.55515e-004

6.4 Couette Entry Profile

We begin again with the Darcy-Forchheimer-Brinkman equation and simply substitute $C = 0$ in (27) giving us

$$u_{yy} - \kappa^2 u - \kappa R C_d u^2 = 0 \tag{57}$$

subject to the following boundary conditions

$$u_1(0) = 0, \quad u_1(1) = 1 \tag{58}$$

This leads to the following OHAM solution

$$\tilde{u}(y) = u_0 + u_1 \tag{59}$$

where

$$u_0(y) = \alpha_0 e^{\kappa y} + \beta_0 e^{-\kappa y}$$
$$u_1(y) = A_1 e^{\kappa y} + B_1 e^{-\kappa y} + C_1 e^{2\kappa y} + D_1 e^{-2\kappa y} + G_1 \tag{60}$$

where

$$\alpha_0 = \frac{1}{2\sinh(\kappa)}, \quad \beta_0 = \frac{-1}{2\sinh(\kappa)}$$

and

$$A_1 = \frac{1}{2\sinh(\kappa)}[C_1(e^{-\kappa} - e^{2\kappa}) + D_1(e^{-\kappa} - e^{-2\kappa})$$
$$+G_1(e^{-\kappa} - 1)]$$
$$B_1 = \frac{1}{2\sinh(\kappa)}[C_1(e^{2\kappa} - e^{\kappa}) + D_1(e^{-2\kappa} - e^{\kappa})$$
$$+G_1(1 - e^{\kappa})]$$
$$C_1 = -\frac{RC_d\lambda\alpha_0^2}{3\kappa^2}, \quad D_1 = -\frac{RC_d\lambda\beta_0^2}{3\kappa^2}$$
$$G_1 = \frac{2\alpha_0\beta_0 RC_d\lambda}{\kappa^2}. \tag{61}$$

Furthermore, as done earlier with $C = 0$, $R = 1$, $\kappa = 1$ and $C_d = 0.55$ we get

$$\lambda = -0.97377373728.$$

Then, we obtain

$$\tilde{u}(y) = 0.27997542579534e^{y} - 0.53850190998946e^{-y} +$$
$$0.03231581052427e^{2y} + 0.03231581052427e^{-2y}$$
$$+0.19389486314559 \tag{62}$$

We once again substitute $C_d = 0$ into (70) giving us the DLB solution

$$u(y) = \frac{\sinh(y)}{\sinh(1)} \tag{63}$$

which is the expected solution if we solve the Darcy–Lapwood–Brinkman equation (43) with $C = 0$. This further verifies the solutions presented in the preceding sections.

In Fig. 3 we present once again the graphs of the solutions for the two models for a Couette entry profile.

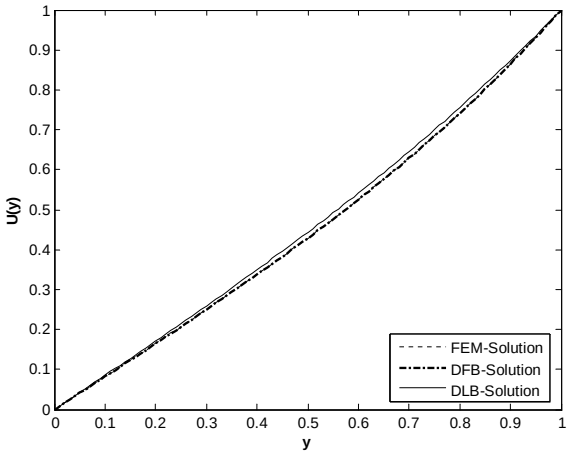

Figure 3: This graph represents a Couette type entry profile. Variation of velocity u versus y for both the Darcy-Lapwood-Brinkman (DLB) and Darcy-Forchheimer-Brinkman (DFB) models. In addition, the benchmark FEM solution is also shown. For computing these graphs we have set $C = 0, R = 1$ and $k = 1$. In addition, for the DFB model $C_d = 0.55$ and for the DLB model $C_d = 0$

Once again we notice the slower profile of the Darcy-Forchheimer-Brinkman model, due to the presence of the microscopic inertia. The graph matches closely with the results of [1].
Table 3 illustrates the $\mathcal{L}^2$-norm of the error between the *zeroth-order* and *first-order* solutions and the FEM-benchmark solution. we can see that the error is decreasing with respect to the order of OHAM solution and therefore the optimal homotopy perturbation metho provides a good approximation of the exact solution.

Table 3: The $\mathcal{L}^2$-norm of the error between the FEM-solution and OHAM-solutions for Couette type entry profile.

Δy	0.01
Approximation degree p	4
$\|\|U_{FEM} - u_0\|\|_{\mathcal{L}^2(0,1)}$	0.00806
$\|\|U_{FEM} - \tilde{u}\|\|_{\mathcal{L}^2(0,1)}$	8.30773e-005

6.5 Further Error Analysis

In this section, we present the efficiency of the OHAM by showing the absolute error $\mathcal{E}rror$ for the different cases of flows, this error is defined by

$$\mathcal{E}rror\left(\tilde{u}\right) = \left| \int_0^1 \left[L\left(\tilde{u}\left(y\right)\right) + N\left(\tilde{u}\left(y\right)\right) + g\left(y\right) \right] dy \right| \quad (64)$$

where $\tilde{u}$ is the approximate OHAM solution.

6.5.1 Poiseuille Entry Profile

We developed in (46) and (49) respectively the zeroth and the first order OHAM solutions of the Darcy-Forchheimer-Brinkman equation as

$$u_0(y) = 5 - 3.65529e^{-y} - 1.34471e^{y} \quad (65)$$

$$\tilde{u}(y) = 5.42216e^{y} + 5.16871e^{-y} + 0.31562e^{2y} + 2.33214e^{-2y} - 3.5207ye^{y} + 9.57025ye^{-y} - 18.23863 \quad (66)$$

We show now the absolute errors in Table 4 to see the performance of the OHAM.

6.5.2 Poiseuille–Couette Entry Profile

We developed in (60) and (54) respectively the zeroth and the first order OHAM solution of the Darcy-Forchheimer-Brinkman equation as

$$u_0(y) = 5 - 4.08075e^{-y} - 0.919248e^{y} \quad (67)$$

$$\tilde{u}(y) = 4.45372e^{y} + 4.10178e^{-y} + 0.14316e^{2y} + 2.82132e^{-2y} - 2.33612ye^{y} + 10.370611ye^{-y} - 16.52 \quad (68)$$

We show now the absolute errors in Table 5 to see the performance of the OHAM method.

6.5.3 Couette Entry Profile

We developed in (59) the zeroth and the first order OHAM solution of the Darcy-Forchheimer-Brinkman equation as

$$u_0(y) = -0.425459e^{-y} + 0.425459e^{y} \quad (69)$$

$$\tilde{u}(y) = 0.27997e^{y} - 0.5385e^{-y} + 0.032315e^{2y} + 0.03231e^{-2y} + 0.19389 \quad (70)$$

We show now the absolute errors in Table 6 to see the performance of the OHAM method.

Table 4: The Absolute errors for Poiseuille type entry profile.

$\mathcal{E}rror\left(u_0\right)$	$\mathcal{E}rror\left(\tilde{u}\right)$
0.0944954	0.000136731

Table 5: The Absolute errors for Poiseuille–Couette type entry profile.

$\mathcal{E}rror\,(u_0)$	$\mathcal{E}rror\,(\tilde{u})$
0.44592	0.000660028

Table 6: The Absolute errors for Couette type entry profile.

$\mathcal{E}rror\,(u_0)$	$\mathcal{E}rror\,(\tilde{u})$
0.161968	0.00156923

6.5.4 Comments

Thus in these subsections for each of the cases investigated in this paper we have demonstrated that using the OHAM as we go from the zeroth order to higher order solutions it leads to a significant decrease in the errors as one would expect in an efficient method that is converging to a solution. This further consolidates our results regarding the accuracy and convergence of the OHAM.

7 Conclusions

The main objective of this paper was to present an approximate analytical solution of the particular form of the Darcy-Forchheimer-Brinkman model, representing the developed flow through a porous channel between parallel plates. The problem has been well documented [1], in fact we follow the analysis of this work and use it as a bench mark for the analytical solution presented here. We have further reenforced this with a highly accurate numerical solution. We have considered three types of entry profiles driving the flow namely, Poiseuille, Couette and Poiseuille–Couette type. In addition, we have considered the problem with generalised boundary conditions and presented the solution with respect to these boundary conditions. The solution simply requires the input of the appropriate parameters to produce solutions to different problems. We have demonstrated this through the subsections above in the section on Results and Analysis. Although we do not really present the solution to a new problem, we have used this problem as a demonstration of the OHAM as an effective method for solving nonlinear problems.

Physically, as expected this solution shows for instance not only the overall effect of the microptic inertia, but additionally shows the term(s) (since more terms in the solution can be taken) that contribute to the dynamics of the problem. The paper also demonstrates the advantages of an analytical solution. As verification, we have shown the solution of the Darcy-Lapwood-Brinkman model for the same problem; the model can be obtained from the Darcy-Forchheimer-Brinkman model by simply setting the drag coefficient to zero. As such the solution obtained by doing the same with our solution we expect the correct solution of the Darcy-Lapwood-Brinkman model, which is an easier linear solvable differential equation; and this in fact was shown and verifies in a manner our solution. In addition, we have offered further verification of the solution by comparing to the solution of [1], and all scenarios show a match. And finally, we have compared the solution to an accurate numerical solution and not only have we shown the solution matches and is indeed accurate, but we have also demonstrated the convergence of the OHAM.

Finally, it is worth noting that the solution presented in this paper compares well with the HPM solution of [6] thus showing as stated at the onset that the HPM can be accurate for certain problems.

References

[1] M. M. Awartani and M. H. Hamdan, Fully developed flow through a porous channel bounded by flat plates, Applied Mathematics & Computation, 169, 749-757, (2005)

[2] S. J. Liao and A. T. Chwang, Application of homotopy analysis method in nonlinear oscillations, ASME Journal Applied Mechanics, 65, 914, (1998)

[3] J.H. He, Homotopy perturbation technique, Computer Methods in Applied Mechanics and Engineering, 178, 257-262, (1999)

[4] J. Biazar and H. Ghazvini, Convergence of the homotopy perturbation method for partial differential equations, Nonllinear Analysis: Real World Applications, 10, 2633-2640, (2009)

[5] Vasile Marinca and Nicolae Herişanu and Constantin Bota and Bogdan Marinca, An optimal homotopy asymptotic method applied to the steady flow of a fourth-grade fluid past a porous plate, Applied Mathematics Letters, 22, 245251, (2009)

[6] A. R. Ansari and A. M. Siddiqui, An Analytical solution of the Darcy-Forchheimer-Brinkman equation for fully developed through prous channel bounded by flat plates, Journal of Porous Media, 14, (2011)

[7] M. H. Hamdan, Single-phase flow through porous channels, a review of flow models and channel entry conditions, Applied Mathematics & Computation, 62, 203-222, (1994)